JVI Journals.ASM.org

Inefficient Type I Interferon-Mediated Antiviral Protection of Primary Mouse Neurons Is Associated with the Lack of Apolipoprotein L9 Expression

Marguerite Kreit,[a] Sophie Paul,[a]* Laurent Knoops,[a,b] Aurélie De Cock,[a] Frédéric Sorgeloos,[a] Thomas Michiels[a]

Université Catholique de Louvain, de Duve Institute, Brussels, Belgium[a]; Hematology Unit, Cliniques Universitaires Saint-Luc, Brussels, Belgium[b]

ABSTRACT

We examined the antiviral response promoted by type I interferons (IFN) in primary mouse neurons. IFN treatment of neuron cultures strongly upregulated the transcription of IFN-stimulated genes but conferred a surprisingly low resistance to infection by neurotropic viruses such as Theiler's murine encephalomyelitis virus (TMEV) or vesicular stomatitis virus (VSV). Response of primary mouse neurons to IFN treatment was heterogeneous, as many neurons failed to express the typical IFN response marker Mx1 after IFN treatment. This heterogeneous response of primary neurons correlated with a low level of basal expression of IFN-stimulated genes, such as *Stat1*, that are involved in signal transduction of the IFN response. In addition, transcriptomic analysis identified 15 IFN-responsive genes whose expression was low in IFN-treated primary neurons compared to that of primary fibroblasts derived from the same mice (*Dhx58*, *Gvin1*, *Sp100*, *Ifi203* isoforms 1 and 2, *Irgm2*, *Lgals3bp*, *Ifi205*, *Apol9b*, *Ifi204*, *Ifi202b*, *Tor3a*, *Slfn2*, *Ifi35*, *Lgals9*). Among these genes, the gene coding for apolipoprotein L9b (*Apol9b*) displayed antiviral activity against Theiler's virus when overexpressed in L929 cells or in primary neurons. Accordingly, knocking down *Apol9b* expression in L929 cells increased viral replication. Therefore, we identified a new antiviral protein induced by interferon, ApoL9b, whose lack of expression in primary neurons likely contributes to the high sensitivity of these cells to viral infection.

IMPORTANCE

The type I interferon (IFN) response is an innate immune defense mechanism that is critical to contain viral infection in the host until an adaptive immune response can be mounted. Neurons are a paradigm for postmitotic, highly differentiated cells. Our data show that primary mouse neurons that are exposed to type I interferon remain surprisingly susceptible to viral infection. On one hand, the low level of basal expression of some factors in neurons might prevent a rapid response of these cells. On the other hand, some genes that are typically activated by type I interferon in other cell types are expressed at much lower levels in neurons. Among these genes is the gene encoding apolipoprotein L9, a protein that proved to have antiviral activity against the neurotropic Theiler's murine encephalomyelitis virus. Our data suggest important functional differences in the IFN response mounted by specific cell populations.

Neurons are among the most sophisticated examples of differentiated cells. They play a critical role in the coordination of body functions. Yet, apart from cells of the olfactory pathway, neurons are poorly renewable in the adult brain. Cytolytic clearance of pathogens infecting neurons could thus be extremely deleterious for the host. Fortunately, neurons were reported to have evolved noncytolytic strategies, such as gamma interferon (IFN-γ) and antibody-mediated viral replication inhibition, to limit viral spread (1).

Type I interferons (also named IFN-α/β and referred to hereafter as IFN) are first-line antiviral cytokines that are expected to contribute to the antiviral defense of neurons. Experimental infections of mice that are deficient for the IFN receptor (IFNAR) have highlighted the highly protective role of IFN against viral infections of the central nervous system (CNS) (for a review, see references 2 and 3). In humans, mutations in genes of the IFN pathway have been associated with high susceptibility to herpes simplex virus 1 encephalitis (4, 5). *In vitro* and *in vivo* studies suggest that neurons can take part in the innate immune response through their ability to produce IFN and to respond to this cytokine (6–10). However, both IFN production and IFN response appear to be more restricted in neurons than in other cell types. Kallfass et al. (11) elegantly showed that after infection with the highly neurotropic La Crosse virus, IFN-producing cells included very few neurons. Instead, astrocytes and microglial cells were mostly responsible for IFN production, despite these cells not being detectably infected. The response of neurons to IFN is also somehow restricted and displays regional specificity. A recent study reported that rat hippocampal neurons did not mount a protective response against Borna disease virus after IFN-α treatment (12). Analysis of transgenic mice overexpressing IFN-α in the CNS revealed that CA1 and CA2 but not CA3 neurons of the hippocampus responded by expressing the IFN-inducible Mx1 gene (13). Recently, Cho et al. reported an important difference in responsiveness between granule cell neurons of the cerebellum

Received 15 October 2013 Accepted 14 January 2014
Published ahead of print 22 January 2014
Editor: B. Williams
Address correspondence to Thomas Michiels, thomas.michiels@uclouvain.be.
* Present address: Sophie Paul, Cardio3 BioSciences, Mont-Saint-Guibert, Belgium.
Supplemental material for this article may be found at http://dx.doi.org/10.1128/JVI.03018-13.

doi:10.1128/JVI.03018-13

and cortical neurons. Neurons from the cerebellum had a higher basal expression level of IFN-stimulated genes (ISG) and responded more strongly to IFN treatment (14).

In this work, we analyzed the IFN response in primary cortical and hippocampal mouse neurons. Our results show that mouse primary neurons treated with IFN were inefficiently protected against Theiler's murine encephalomyelitis virus (TMEV) or vesicular stomatitis virus (VSV) infection, despite a strong transcriptional activation of ISG. Transcriptomic analysis identified 15 IFN-responsive genes whose expression was low in IFN-treated primary neurons compared to that of primary fibroblasts. Among them, the gene encoding apolipoprotein L9b (*Apol9b*) was found to contribute to antiviral resistance.

MATERIALS AND METHODS

Mice. 129/Sv, C57BL/6, CD1, and IFNAR-I-KO 129/Sv mice were purchased from Charles River Laboratories or from the animal facility of the University of Louvain (Brussels). B6.A2G-Mx1 mice carrying functional *Mx1* alleles (15) were from the breeding colony maintained in Freiburg, Germany. Handling of mice and experimental procedures were conducted in accordance with national and institutional guidelines for animal care and use (agreement reference 2010/UCL/MD/031).

Cell culture. L929 cells (ATCC), Neuro-2A (ECACC), LKR-10 (16, 17), and 293T cells (18) were maintained in Dulbecco's modified Eagle medium (Lonza) supplemented with 10% fetal calf serum (FCS) (Sigma) and 100 U/ml of penicillin-streptomycin (Lonza). BHK-21 cells (ATCC) were cultured in Glasgow's modified Eagle's medium (Sigma) supplemented with 10% newborn bovine serum (Gibco), 100 U/ml of penicillin-streptomycin (Lonza), and 2.6 g of tryptose phosphate broth per liter (Difco).

Primary mixed hippocampal/cortical neuronal cultures were prepared from embryonic day 14.5 (e14.5) pregnant mice (19). Except when otherwise stated, primary neurons were derived from CD1 mice. Briefly, hippocampi and cortices from e14.5 mouse embryos were harvested and dissociated in Krebs buffer (10× Krebs is 120.9 mM NaCl, 4.83 mM KCl, 1.22 mM KH_2PO_4, 25.5 mM $NaHCO_3$, 13 mM L-glucose) containing 3 g of bovine serum albumin (BSA; Sigma) and 0.304 g of $MgSO_4$ per liter and 2 mM HEPES (*N*-2-hydroxyethylpiperazine-*N*N-2- ethanesulfonic acid) buffer and were incubated successively with trypsin and DNase (Sigma). Dissociated cells were then pelleted by low-speed centrifugation and resuspended in neurobasal medium (Invitrogen) supplemented with 2% B27 (Invitrogen), 1% GlutaMAX (Invitrogen), 4 g per liter of BSA (Sigma), and 100 U/ml of penicillin-streptomycin (Lonza). Next, 100,000 neurons were seeded on 13-mm glass coverslips coated overnight with polyornithine (0.5 mg/ml; Sigma) and for 4 h with 1% laminin (Roche). Half of the medium was replaced after 1 day. For pure hippocampal neuronal cultures, the protocol of Fath et al. (20) was used. On one hand, brain cells were prepared as described above to provide feeding cells. On the other hand, hippocampi were isolated and dissociated, and hippocampal neurons were seeded on polyornithine- and laminin-coated coverslips. The coverslips were then placed in 12-well plates in which feeding cells (100,000 cells/well) had been seeded as an outer ring around the coverslip. The number of seeded hippocampal neurons per coverslip was 10,000 for immunolabeling, 80,000 for flow cytometry analysis, and 100,000 for reverse transcription-quantitative PCR (RT-qPCR) analysis. Mouse embryonic fibroblasts (MEFs) were prepared as described previously (21) and routinely divided for up to 8 passages.

Interferon and viruses. IFN-β was produced as described previously from 293T cells transfected with pcDNA3-IFN-β (22). IFN-β was diluted in culture medium. Unless otherwise indicated, 5 units of IFN per ml were used for treatment. For control treatment of cells (mock), supernatant collected from 293T cells transfected with the empty pcDNA3 vector was used and diluted in culture medium as for IFN-β. The interferon antiviral activity was quantified by a cytopathic effect reduction assay as described previously (23). IFN-λ was quantified by the same method using LKR-10 cells, which readily respond to IFN-λ. One unit was taken as the amount of IFN-λ that protected 50% of the cells against viral infection.

TABLE 1 Recombinant viruses and lentiviral vectors used in the study

Virus name[a]	Parental virus/vector[b]	Characteristics[c]
KJ6	TMEV (DA1)	Capsid adapted to infect L929 cells
TM659	KJ6	Zn finger mutation in L protein capsid adapted to infect L929 cells
KJ7	KJ6	GFP-coding sequence replacing codons 5–67 of L capsid adapted to infect L929 cells
SD1	TMEV (GDVII)	Zn finger mutation in L protein; efficient at infecting *in vitro*-cultured neurons
KJ26	TMEV (GDVII)	GFP-coding sequence replacing codons 1–67 of L; efficient at infecting *in vitro*-cultured neurons
VSV-GFP	VSV	GFP-coding sequence
pTM941	pCCLsin	Lentiviral vector (PGK-MCS-IRES-eGFP)
pTM942	pCCLsin	Lentiviral vector (PGK-MCS-IRES-mCherry)
pMK44	pTM942	*ApoL9* expression
pMK46	pTM942	*Dhx58* expression
pMK42	pTM942	*Tor3a* expression
pMK50	pTM942	*SP100* expression
pMK51	pTM942	*Irgm2* expression
pMK53	pTM942	*Ifi202b* expression
pMK56	pTM942	*Ifi203* expression
pMK43	pTM942	*Lgals9* expression
pMK84	pLKO.1	mCherry-coding region replacing puro^R
pMK74	pMK84	shRNA targeting *Apol9b* coding region
pMK75	pMK84	shRNA targeting *Apol9b* 3′ UTR

[a] Plasmids used to produce the listed viruses by reverse genetics have a "p" before the virus name (e.g., pKJ6 for virus KJ6).
[b] pCCLsin, pCCLsin.PPT.hPGK.GFP.pre.
[c] L, leader protein of Theiler's virus; PGK, human phosphoglycerate kinase promoter; MCS, multicloning site; eGFP, enhanced GFP; puro^R, puromycin resistance-coding region.

Theiler's murine encephalomyelitis viruses (TMEV or Theiler's virus) used in this study were derived from the persistent DA strain (24) and from the neurovirulent GDVII strain (25). TMEV derivatives were produced as previously described from the corresponding full-length cDNA clones (26, 27). SD1 is a mutant of the GDVII strain carrying a zinc finger mutation in the IFN antagonist leader protein (28). KJ26 was constructed by substituting the enhanced green fluorescent protein (eGFP) coding sequence for codons 1 to 67 of the L-coding region of virus GDVII. DA1 derivatives carrying capsid mutations that enhance L929 cell infection (29) were KJ6, equivalent to the DA1 virus, and KJ7, a derivative of KJ6 carrying the GFP coding sequence between codons 5 and 67 of the L-coding region (21).

VSV (Indiana strain) was a gift from Eliane Meurs (Pasteur Institute, Paris, France). The VSV derivative expressing GFP was a gift from Martin Schwemmle (University of Freiburg, Germany). Viruses were propagated and titrated on BHK-21 cells. Table 1 presents the viruses used in this study.

Construction of lentiviral vectors and cell transduction. The coding sequence of the 14 ISG of interest were PCR amplified from C57BL/6 mouse spleen cDNA, using Phusion polymerase (New England BioLabs), and cloned in pTM941 and pTM942, using AgeI/BsiWI or BamHI/SmaI restriction sites introduced in the PCR primers (see Table S1 in the supplemental material). pTM941 and pTM942 are bicistronic lentiviral vec-

tors derived from pCCLsin.PPT.hPGK.GFP.pre (30) and carrying a phosphoglycerate kinase promoter, a multicloning site, the internal ribosome entry site (IRES) of TMEV (31), and the eGFP- or mCherry-coding sequences, respectively. The cloned ISG open reading frames were sequenced to ensure that the PCR amplification step did not introduce unexpected mutations. Lentivirus particles were generated by transient transfection of 293T cells grown in 75-cm^2 Petri dishes by the calcium phosphate method, using 7.5 μg of lentiviral vector, 2.25 μg of pMD2-VSV-G (VSV-glycoprotein), 3.375 μg of pMDLg/pRRE (Gag-Pol), and 1.875 μg of pRSV-Rev (Rev) (30). Cell supernatants, harvested at 24 and 48 h, were passed through a 0.45-um filter and concentrated 10 times using either Lenti-X concentrator (Clontech) for use on fibroblasts or Vivaspin columns (cutoff, 1,000,000 Da; Vivaspin) for use on neurons. Cells were transduced with lentiviral particles 3 to 6 days before infection with TMEV derivatives.

RNA interference. pMK84 is a pLKO.1 (32) derivative constructed by substituting the mCherry-coding region for that of the puromycin resistance gene. To this end, mCherry was amplified by PCR with primers introducing BamHI and KpnI restriction sites. Short hairpin RNA (shRNA) sequences targeting the mouse *ApoL9b* transcript were selected from the RNA mission collection (Sigma) and cloned in pMK84 using AgeI and EcoRI restriction sites introduced in the PCR primers according to the Addgene protocol. shRNA (TRCN0000346551), which targets the 3′ end of *Apol9*, gave a more complete inhibition than shRNA (TRCN0000346484), which targets the *Apol9* coding sequence (data not shown), and was used for subsequent knockdown experiments. Lentiviral particles were generated as described above by transfecting 293T cells with 7.5 μg of vector plasmid DNA, 5.5 μg of psPAX2 (Addgene), and 2.25 μg of pMD2-VSV-G. The efficiency of RNA silencing was assayed 3 days after transduction by measuring *ApoL9b* gene expression (RT-qPCR) in L929 cells after IFN-β stimulation (data not shown).

RNA extraction and quantitative RT-qPCR. Total RNA preparations, RT, and quantitative PCRs (qPCR) were performed as previously described (33). qPCR standards consisted of 10-fold dilutions of quantified plasmid DNA carrying the sequence to be amplified: pTM793 for β-*actin*, pMK72 for *Apol9b*, pCS40 for *Oasl2*, pSPA31 for *Stat1*, pSPA41 for *Ifit3*, pSPA38 for *Adar1*. These plasmids are derivatives of pCR4-ToPo (Invitrogen) in which the corresponding PCR fragments were cloned. For TMEV cDNA quantification, we used pTM410, a pTZ19R derivative carrying nucleotides 1 to 1,730 of TMEV (DA1). For VSV cDNA quantification, we used pMD2-VSV-G. Primer sequences are given in Table S2 in the supplemental material.

Immunolabelings and microscopy. Prior to immunolabeling, neurons were fixed for 10 to 15 min in 300 μl of phosphate-buffered saline (PBS) containing 4% paraformaldehyde (PFA). Cells were then washed in 500 μl of PBS and permeabilized for 5 min at room temperature in 500 μl of PBS containing 0.1% Triton X-100. Blocking occurred for 1 h at room temperature in 200 μl of TNB blocking reagent (PerkinElmer). Cells were next incubated with the primary antibody diluted in TNB at the following dilutions: microtubule-associated protein 2 (MAP2; rabbit [reference no. 188002] or guinea pig [reference no. 188004] polyclonal antibody; Synaptic Systems), 1/1,000; VP1 of TMEV (mouse monoclonal F12B3 antibody kindly provided by M. Brahic),1/50; Mx1 (rabbit polyclonal antibody kindly provided by P. Stäheli) (34), 1/150; TUJ-I (mouse monoclonal antibody [reference no. MMS-435P]; Covance), 1/500; and STAT1 (rabbit polyclonal antibody [reference no. sc-346]; Santa Cruz), 1/100. After1 h of incubation at room temperature, cells were washed 3 times for 5 min in 500 μl PBS. Alexa Fluor-conjugated secondary antibodies (Invitrogen) were incubated for 1 h at a 1/800 dilution in TNB. Finally, cells were washed 3 times in 500 μl PBS and mounted with Mowiol for fluorescence microscopy. For nuclear staining, cells were incubated for 5 min in Hoechst 33258 before the final washing steps. Fluorescence microscopy was performed using a DMIRB inverted microscope (Leica) equipped with a DC200 digital camera (Leica) or a spinning-disk confocal microscope equipped with an Axiocam MRm camera (Zeiss). Intensity, contrast, and color balance of images were equilibrated using ImageJ or Adobe Photoshop.

Flow cytometry. After dissociation, cells were suspended in PBS buffer containing 5% FCS and 0.5% paraformaldehyde. Data acquisition was done with an LSRFortessa flow cytometer (BD Biosciences) using FACSDiva software. Data were analyzed using FlowJo 9.6.4. In cells transduced with mCherry-expressing vectors, viral replication (GFP fluorescence) was measured in the mCherry-positive-gated population. In control mock-transduced cells, viral replication (GFP fluorescence) was measured in the total cell population. The rate of infection was defined as the percentage of GFP-positive cells. Viral replication was estimated by the geometric mean GFP fluorescence intensity in the GFP-positive population. "Normalized infection efficiency" was calculated by combining the rate of infection and viral replication (percent GFP-positive cells multiplied by geometric mean GFP fluorescence of these cells in the mCherry-positive population).

Microarray analysis. Affymetrix pangenomic mouse 430 2.0 microarrays were used to measure gene expression after IFN stimulation in neurons, MEFs, and L929 cells. Two hundred nanograms of RNA was used to synthesize biotinylated amplified RNA (aRNA) according to Affymetrix protocol (GeneChip 3′ IVT Express kit) before hybridization on chips for 16 h at 45°C. GeneChips were washed and stained in an Affymetrix Fluidics Station 450. Hybridized aRNA was detected using streptavidin coupled to phycoerythrin. GeneChips were scanned using a GeneChip Scanner 3000 7G and a GeneChip operating system (GCOS; Affymetrix, Santa Clara, CA). Default values were used to generate raw data. All intensity values were scaled to an average value of 100 per chip according to the method of global scaling implemented in MAS 5.0 software (Affymetrix). For data analysis, all probe set intensities below 20 were set to 20 to exclude unreliable variation related to poorly expressed genes. Genes induced at least 3 times by IFN-β stimulation, in MEFs or in L929 cells, and 1.5 times in the other cell type were considered ISG.

Statistical analyses. Statistical significance was calculated for at least 3 replicates, using the Student *t* test. (*, $P < 0.05$; **, $P < 0.01$; ***, $P < 0.001$).

Microarray data accession number. All microarray data are publicly available through the Gene Expression Omnibus (GEO) database under accession no. GSE53951. Raw data can be downloaded, or users can run the GEO2R software (http://www.ncbi.nlm.nih.gov/geo/geo2r) to compare two or more groups of samples.

RESULTS

ISG transcriptional induction in primary mouse neurons treated with type I IFN. The antiviral response triggered by IFN was analyzed in primary cultures of e14.5 embryonic mixed cortical/hippocampal neurons. After 4 to 6 days of *in vitro* growth (DIV), primary neurons expressed MAP2 (Fig. 1A). Cultures typically contained less than 5% of glial fibrillary acidic protein (GFAP)-positive astrocytes (data not shown).

Primary neurons were treated with increasing doses of IFN-β and the IFN response was assessed by monitoring the expression of *Oasl2*, a strongly induced ISG. In neurons, treatment with 5 U/ml of IFN-β was sufficient to induce a 4-log increase in *Oasl2* expression (Fig. 1B). *Oasl2* mRNA expression was readily induced after 6 h of IFN-β treatment and was maintained during more than 50 h of treatment (Fig. 1C). Response of neurons to IFN-β was confirmed by studying the expression of other ISG like *Stat1*, *Ifit-3*, and *Adar1* (see Fig S1 in the supplemental material). ISG expression levels after IFN treatment were similar in neurons and L929 fibroblasts and slightly lower in mouse embryonic fibroblasts (MEFs). Yet, basal ISG expression levels were generally lower in neurons than in fibroblasts (Fig. 1C to E; see also Fig S1).

IFN-β is inefficient at protecting primary mouse neurons from virus infection. We next tested the antiviral protection of

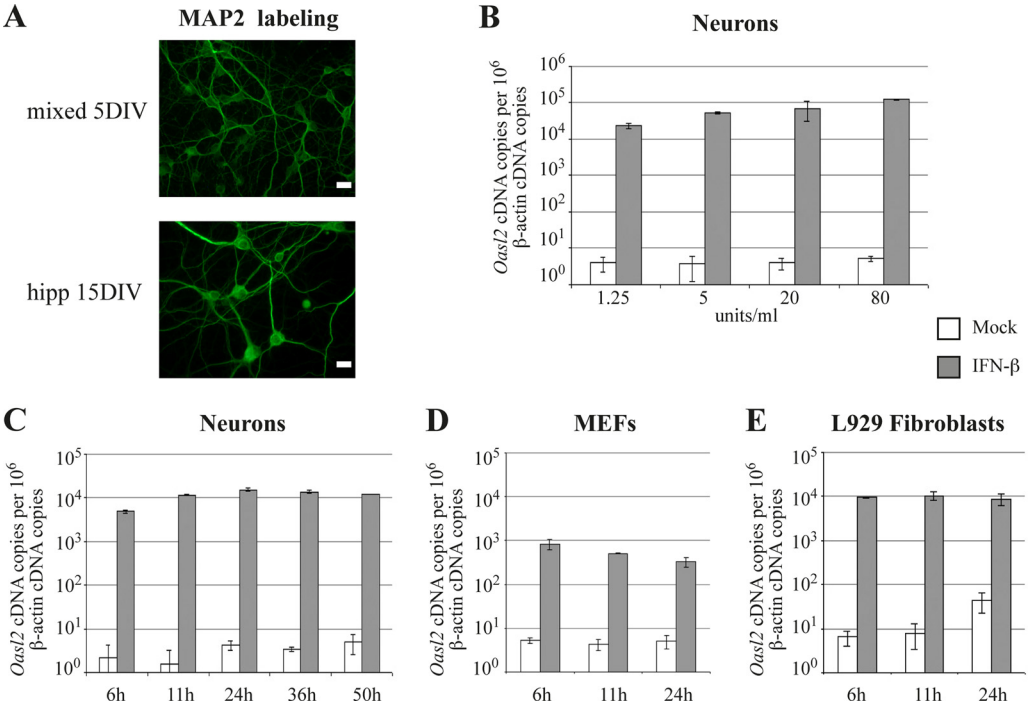

FIG 1 Response of primary neurons and L929 fibroblasts to type I IFN. (A) MAP2 immunolabeling of cultured mixed hippocampal/cortical (mixed) or hippocampal (hipp) primary neurons at 5 and 15 DIV, respectively (scale bar, 10 um). (B to E) *Oasl2* transcripts were quantified by RT-qPCR in mock-treated cells (white columns) and in IFN-β-treated cells (gray columns). (B) Response of mixed neuron cultures to increasing doses of IFN-β (1.25 to 80 units per ml). (C and D) Time course of *Oasl2* expression in 5 DIV primary mixed neurons (C), in MEFs (D), and in L929 cells (E) treated with 5 units/ml of IFN-β or mock treated. Graphs show means and standard deviations (SD) for one representative experiment performed on triplicate cultures.

neurons mediated by the IFN-β treatment. Therefore, primary neurons, MEFs, or L929 cells were treated for 24 h with IFN-β and then infected with 5 PFU per cell of virus SD1. SD1 is a TMEV (GDVII strain) derivative carrying a mutation in the Zn finger of the IFN antagonist leader protein and is very efficient at infecting *in vitro*-cultured neurons (28).

In both primary fibroblasts and fibroblastic L929 cells, IFN-β treatment mediated a strong reduction in viral genome replication, as assessed by RT-qPCR. In contrast, in neurons, SD1 replication hardly decreased after IFN treatment (Fig. 2A). Twenty-four hours after infection, the effect of IFN treatment on viral load was 1,000-fold for L929 cells, 80-fold for MEFs, and only 3-fold for neurons. These experiments were repeated more than 6 times using 4 to 6 DIV neuron cultures at the time of infection and varying the multiplicity of infection, and consistent data were obtained. Immunolabeling of VP1 viral antigen in infected neurons confirmed the surprisingly high susceptibility of IFN-α- or IFN-β-treated neurons to SD1 virus infection (data not shown). Also, assessing infectious virus production in the supernatants of infected neuron and MEF cultures confirmed the inefficient protection provided by IFN-β in neurons (Fig. 2B).

We next compared viral replication in IFN-treated primary neurons derived from wild-type (WT) and type-I IFN receptor-deficient (IFNAR-KO) 129/Sv mice. In agreement with the above data, we observed no significant effect of the lack of type I IFN receptor on SD1 virus replication in these cells (Fig. 2C).

We next tested whether the lack of antiviral protection mediated by IFN treatment in neurons was specific to TMEV or whether it was a more general phenomenon. Therefore, infection experiments were repeated using vesicular stomatitis virus (VSV). As shown in Fig. 2D, VSV mRNA levels, detected by RT-qPCR, were hardly decreased in IFN-treated neurons. In contrast, as in the case of TMEV infection, IFN-β promoted a clear protection against VSV in MEFs (Fig. 2D).

Taken together, our data show that IFN treatment of neurons triggers a surprisingly weak antiviral resistance despite a strong transcriptional upregulation of ISG.

Influence of neuron maturity/differentiation on the antiviral state induced by IFN. It was reported that maturation/differentiation of neuron cell lines affected their susceptibility to Sindbis virus infection and their responsiveness to IFN-γ (35). Therefore, we repeated TMEV and VSV infection experiments in mouse hippocampal neurons maintained at low density for up to 2 weeks (Fig. 1A), using the culture protocol described by Fath et al. (20). Replication of TMEV and VSV was assessed in DIV10-12 neurons and in MEFs derived from the same embryos. Again, IFN-β treatment had little effect on viral replication in neurons, while it restricted viral replication by more than two logs in fibroblasts (Fig. 3).

Heterogeneity of the IFN response in primary hippocampal neurons. We used Mx1-positive mice to assess ISG protein expression in neurons that were treated with IFN. The *Mx1* gene is a well-characterized ISG whose product can easily be detected by both immunoblotting and immunocytochemistry. Western blot analysis confirmed that IFN-β treatment of neuron cultures induced ISG (Mx1 and STAT1) expression at the protein level (Fig. 4C). Immunofluorescent labeling was used to confirm that Mx1 and STAT1 were indeed expressed by MAP2-positive cells (Fig. 4A

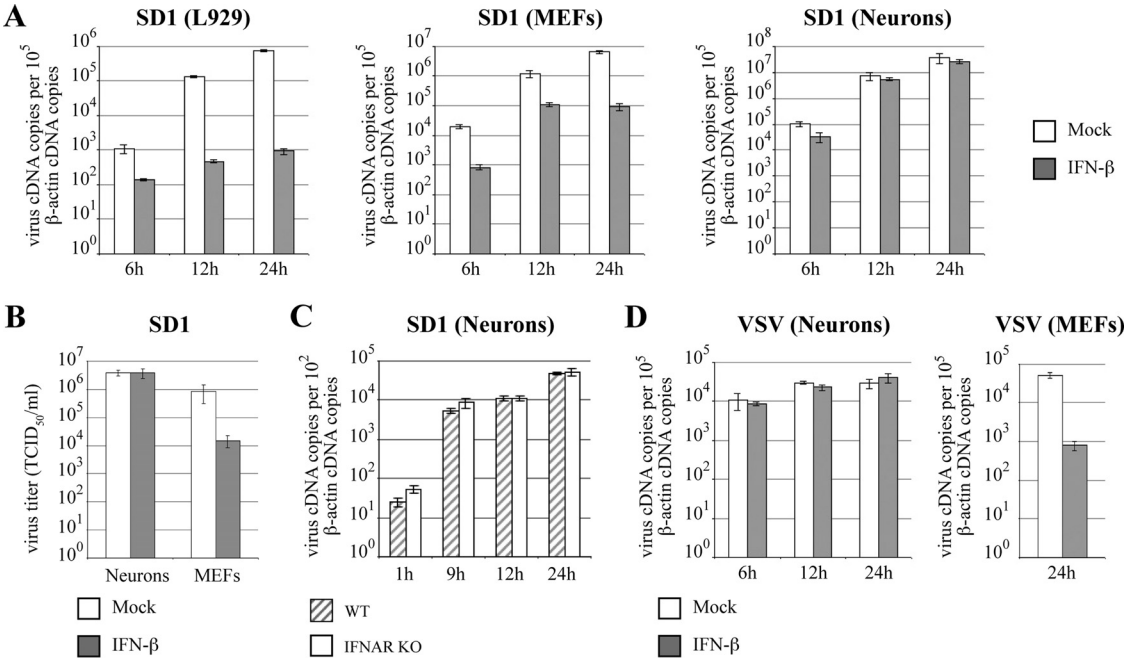

FIG 2 Influence of IFN-β treatment on TMEV and VSV genome replication. (A) Time course of TMEV (SD1) genome replication in L929 cells, MEFs, or mixed neurons that were mock treated (white columns) or treated with 5 units per ml of IFN-β (gray columns). Viral genomes were quantified by RT-qPCR in cells infected for 6, 12, or 24 h with 5 PFU/cell of SD1. (B) Infectious virus production in the supernatants of neurons and MEFs infected for 16 h with SD1. (C) SD1 replication measured by RT-qPCR at the indicated time points in 6 DIV mixed neurons derived from either 129/Sv wild-type mouse embryos (hatched columns) or IFNAR1-deficient mouse embryos (white columns). Neurons were treated with 5 units per ml of IFN-β for 24 h prior to infection with 5 PFU/cell of SD1. (D) VSV genome replication monitored by RT-qPCR in mixed neurons or MEFs that were mock treated (white columns) or treated with 5 units per ml of IFN-β (gray columns) for 24 h prior to infection with 4 PFU per cell of VSV. Graphs show means and SD for one representative experiment performed on triplicate cultures.

and B) and not only by the few glial cells contaminating the culture. Depending on the experiment, the percentage of neurons that became Mx1-positive after IFN-β treatment ranged between 55 and 95% (Fig. 5B).

Next, we tested whether IFN-responsive neurons were protected from viral infection. Therefore, DIV 10–12 neurons from $Mx^{+}/^{+}$ mice were mock treated or treated for 24 h with IFN-β, before being infected with 5 PFU/cell of TMEV (SD1). Twenty-four hours after infection, cells were fixed, immunolabeled for Mx1 (IFN-response), MAP2 (neurons), and VP1 (TMEV) and analyzed by confocal microscopy (Fig. 5A). IFN treatment slightly decreased the rate of infection (Fig. 5C). Yet, protection mediated by the IFN response was weak, as the infection rate only decreased from 65.3% for Mx1-negative neurons to 50.8% for Mx1-positive neurons (Fig. 5D).

Taken together, our data suggest that primary neurons respond heterogeneously to IFN-β treatment and that ISG expression was not sufficient to efficiently protect primary neurons against TMEV infection.

Range of ISG expressed in primary neurons and fibroblasts. Since ISG-expressing neurons were not efficiently protected against TMEV infection, we hypothesized that some ISG that are protective against TMEV infection in fibroblasts might be less expressed in neurons. We thus used transcriptomics to compare gene expression in mock-treated and IFN-β-treated primary neurons and MEFs derived from the same embryos, as well as in L929

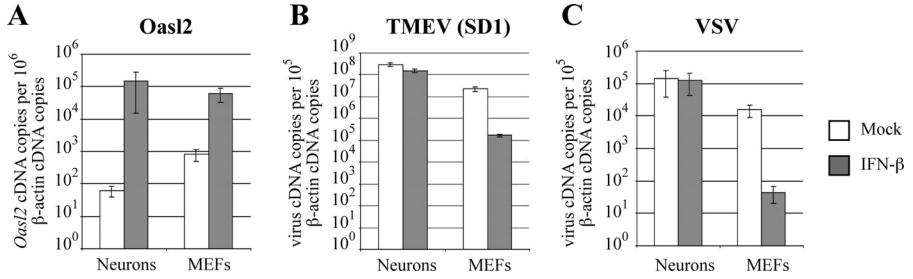

FIG 3 Lack of protection mediated by IFN-β in 12 DIV hippocampal neurons. RT-qPCR analysis of Oasl2 expression (A) and viral replication (B and C) in 12 DIV hippocampal neurons and in MEFs that were mock treated (white columns) or treated with 5 units per ml of IFN-β (gray columns) for 24 h prior to infection. Cells were infected with 5 PFU per cell of TMEV (SD1) (B) or with 4 PFU per cell of VSV (C). Graphs show means and SD from a representative experiment performed in triplicate.

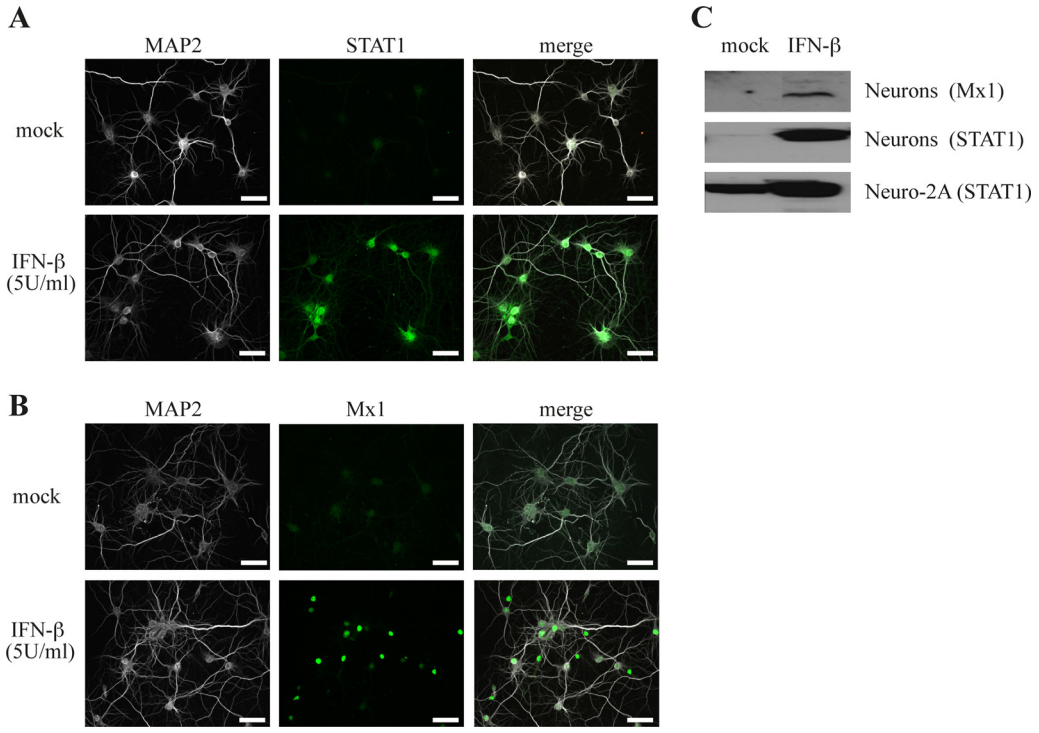

FIG 4 ISG expression in hippocampal neurons. (A and B) DIV10 to DIV 11 neurons derived from $Mx1^{+/+}$ mice were mock treated or treated with 5 units per ml of IFN-β and immunolabeled for the MAP2 neuronal marker (A and B) and for ISG such as *STAT1* (A) and *Mx1* (B). (C) Western blot showing Mx1 and STAT1 induction in neurons and Neuro-2A neuroblastoma cells treated with 5 units per ml of IFN-β.

cells. Microarray data confirmed the overall low basal expression of ISG in neurons. Mean expression of all ISG was 13.86 times lower in untreated neurons than in untreated MEFs. Many genes that were strongly upregulated by IFN-β in MEFs were also strongly upregulated in neurons (Fig. 6A; see also Table S3 in the supplemental material). We failed to identify genes that were upregulated in neurons and not in fibroblasts. Interestingly, we identified 15 genes that were upregulated in fibroblasts and that were not upregulated or were much less expressed in neurons than in fibroblasts: *Dhx58*, *Gvin1*, *Sp100*, *Ifi203* isoforms 1 and 2, *Irgm2*, *Lgals3bp*, *Ifi205*, *Apol9* isoforms a and b, *Ifi204*, *Ifi202b*, *Tor3a*, *Slfn2*, *Ifi35*, and *Lgals9* (Fig. 6B; see also Table S4). These genes are

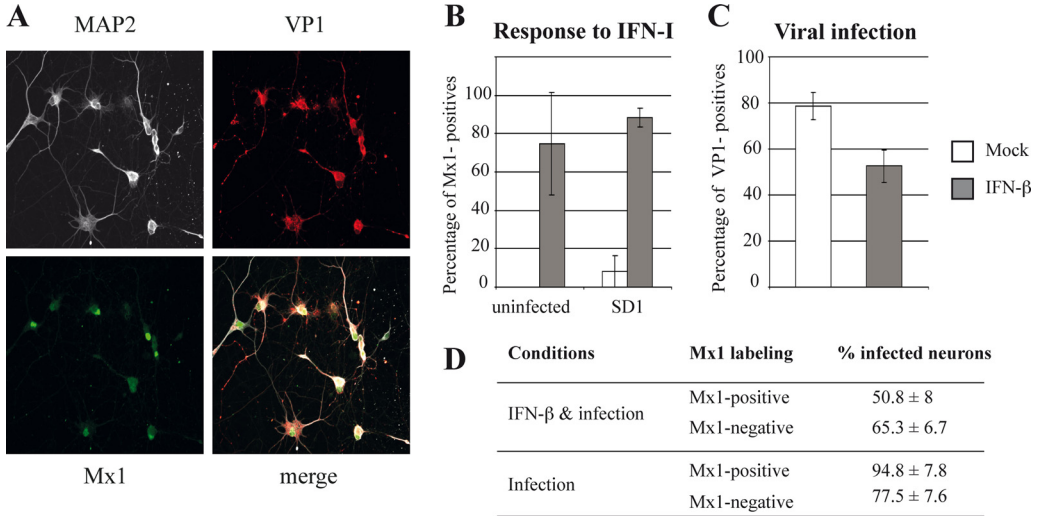

D

Conditions	Mx1 labeling	% infected neurons
IFN-β & infection	Mx1-positive	50.8 ± 8
	Mx1-negative	65.3 ± 6.7
Infection	Mx1-positive	94.8 ± 7.8
	Mx1-negative	77.5 ± 7.6

FIG 5 Heterogeneity of the IFN response in primary neuron cultures. DIV 10 to DIV12 hippocampal neurons derived from $Mx1^{+/+}$ mice were mock treated (white columns) or treated for 24 h with 5 units per ml of IFN-β (gray columns) and infected with SD1 (5 PFU/cell for 24 h) prior to immunolabeling and analysis by confocal microscopy. (A) Illustration of triple immunolabeling with antibodies directed against MAP2 (neurons), VP1 (TMEV capsid), and Mx1 IFN-response. (B and C) Graphs showing the percentage of neurons that respond to IFN treatment by expressing the Mx1 protein (B) and the percentage of infected neurons (C). (D) Percentages ± SD of infected cells in Mx1-negative and Mx1-positive neurons after mock or IFN-β treatment and SD1 infection.

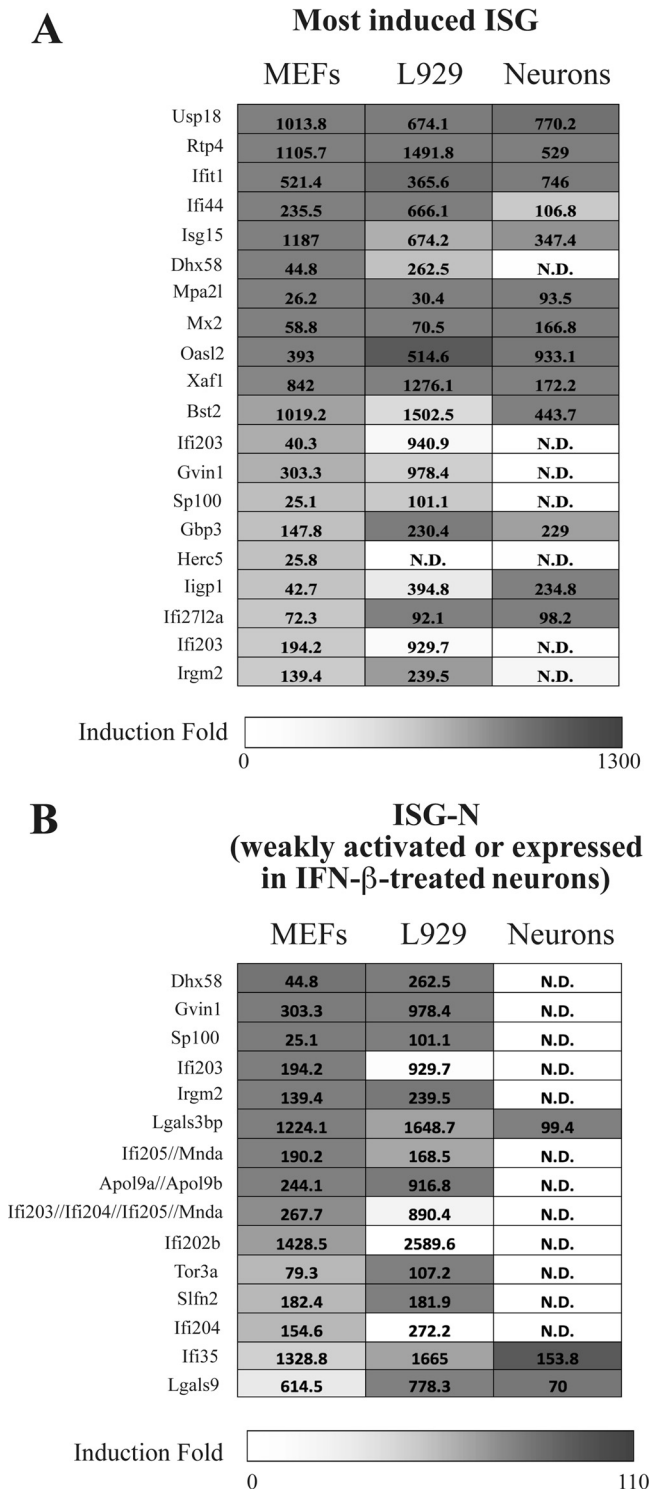

FIG 6 ISG induced in neurons and fibroblasts. Primary mixed neuron cultures (6 DIV), MEFs derived from the same embryos, and L929 cells were either mock treated or treated with 5 U/ml of IFN-β for 24 h. Gene expression was analyzed by microarray (average of $n = 2$ for MEFs and neurons, $n = 1$ for L929 cells). (A) Heat map of 20 genes that showed the highest levels of induction in MEFs following IFN-β treatment. (B) Heat map of ISG that were at least 9-fold-less expressed in neurons than in fibroblasts after IFN-β treatment. Heat map colors refer to the IFN-treated/mock ratio. Numbers in the heat map show the expression level of the gene after IFN-β treatment. ND, not detected (background expression of <20).

further referred to as ISG-N for ISG that are weakly activated or expressed in IFN-β-treated neurons.

Antiviral activity of ISG-N. The coding sequences of 14 ISG-N were amplified by RT-PCR and cloned in the bicistronic lentiviral vectors pTM941 and pTM942, which allow the coexpression of the cloned gene and of eGFP and mCherry, respectively (Fig. 7A). *Gvin1* was excluded from the analysis because the size of its coding region (7.3 kb) was not compatible with lentiviral vector production. In a first screening, L929 cells were transduced with the series of lentiviral vectors coexpressing each ISG and eGFP. Three days after transduction, cells were infected for 8 h with 5 PFU per cell of virus TM659, a TMEV derivative adapted to infect L929 cells and carrying a mutation in the zinc finger of the IFN-antagonist L protein. Cells were immunolabeled for VP1 and analyzed by double fluorescence microscopy (data not shown). This first screening restricted the list to 8 genes having a potential antiviral activity.

In the second screening, the ISG were coexpressed with mCherry from the lentiviral vector pTM942. Transduced L929 cells were then infected for 12 h at 0.1 PFU per cell with KJ07, a TMEV derivative adapted to L929 cells and expressing GFP, which allowed the detection of virus replication by flow cytometry (Fig. 7). One of the ISG showed a reproducible and significant antiviral activity: *Apol9b*, coding the apolipoprotein L9b (Fig. 7B).

We first used RT-qPCR to confirm the low expression level of *ApoL9* in IFN-β-treated neurons as observed by microarray analysis. We also tested whether this gene would be activated in neurons by treatment with IFN-α or IFN-λ. As a control, we analyzed the expression of *Oasl2* and *Usp18*, two ISG that are highly induced in neurons (Fig. 6A). Expression of *Oasl2* and *Usp18* in neurons was readily upregulated by IFN-α and IFN-β but not by IFN-λ. In contrast, *ApoL9* expression was not significantly increased by any of these IFNs (Fig S1D).

Next we generated L929 cell clones that overexpress *Apol9b* to confirm the antiviral activity of this ISG. When these cells were infected with the KJ6 virus strain, adapted to infect L929 cells efficiently, *Apol9b* expression significantly decreased the production of infectious viral particles as measured by plaque assay (Fig. 7C) or by 50% tissue culture infective dose ($TCID_{50}$) quantification (data not shown). *Apol9b* expression in these cells also clearly inhibited replication of KJ26, a GFP-expressing TMEV derivative, as measured by fluorescence-activated cell sorter (FACS) analysis (Fig. 7D).

Apol9b antiviral activity in neurons. The antiviral activity of *Apol9b* was also assayed in neurons. Primary neurons were transduced at DIV 9 with lentiviral vectors coexpressing Apol9b and mCherry (pMK44) or with the empty vector expressing mCherry alone (pTM942). Three days after transduction, neurons were infected for 24 h with 10 PFU per cell of KJ26, a derivative of the neurotropic TMEV strain expressing GFP. Cells were next analyzed by flow cytometry. Expression of *Apol9b* in neurons decreased the percentage of infected cells from 13.8 to 3.8% (Fig. 7E). Moreover, overall infection efficiency, which takes viral replication (mean GFP fluorescence intensity) into account, was also significantly lower in *Apol9b*-expressing cells (Fig. 7F). Analysis of viral replication by RT-qPCR and measurements of infectious virus production confirmed the protective effect of *Apol9b* in neurons, although, in these cases, the differences were not significant (Fig. 7G-H).

Apol9b contributes to resistance of IFN-treated fibroblasts. To evaluate the contribution of *Apol9b* in the antiviral response mediated by IFN in fibroblasts, we used a knockdown strategy.

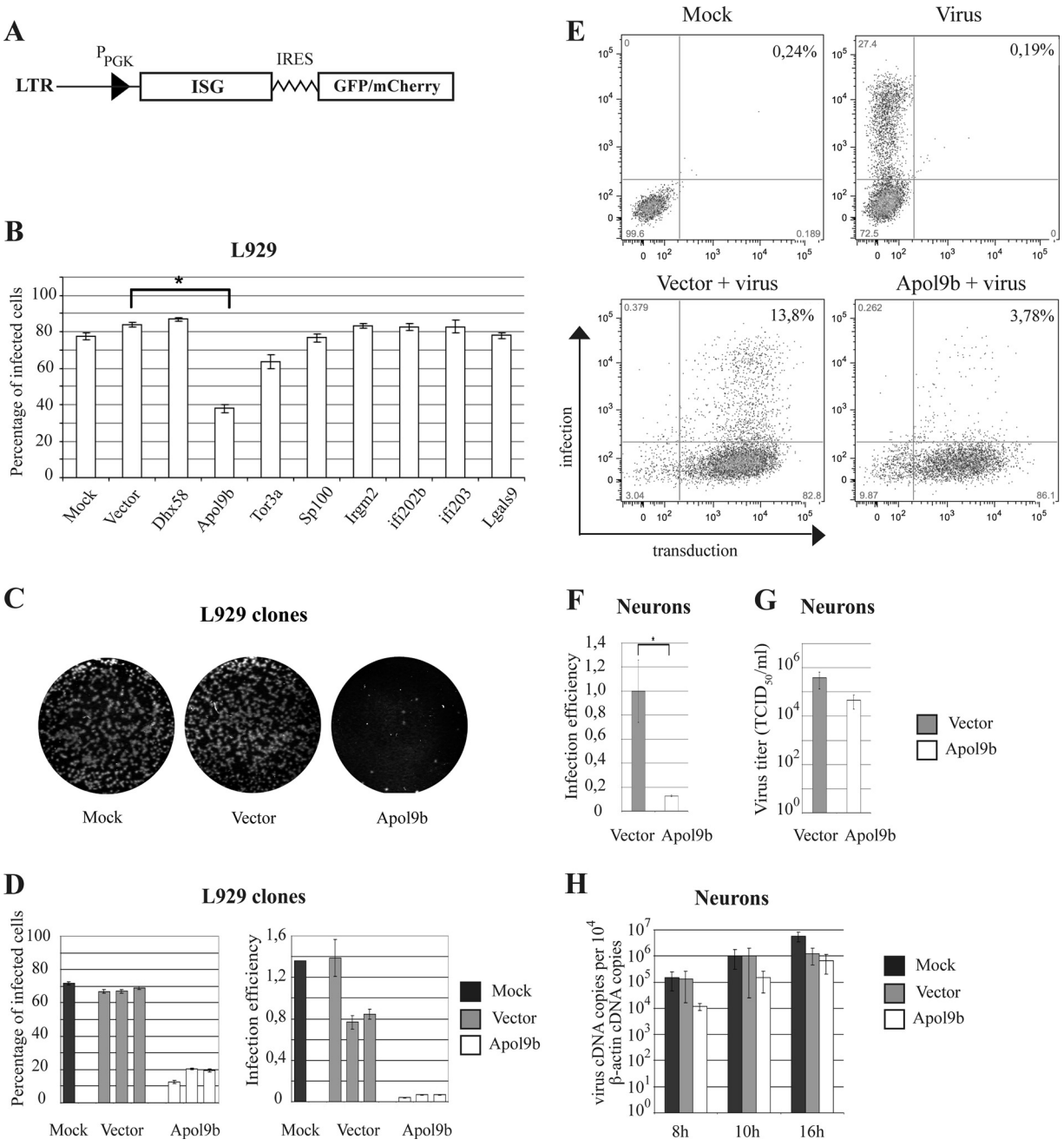

FIG 7 ISG antiviral activity. (A) Schematic representation of lentiviral vectors coexpressing ISG and fluorescent proteins. (B) Screening of the antiviral activity of 8 preselected ISG. Histograms show the percentage of cells that were strongly infected (GFP fluorescence of $>5 \times 10^3$) by KJ7, as monitored by FACS analysis. (C and D) Control L929 cells (mock) and 3 individual clones of L929 cells transduced with the pTM942 vector expressing mCherry alone (empty) or transduced with the vector coexpressing *Apol9*b and mCherry (Apol9b) were infected with TMEV derivatives. (C) Representative plaque assay performed on equal dilutions of supernatants of cells infected for 8 h with the KJ6 virus adapted to infect L929 cells. (D) Histograms showing the percentage of infected cells (left panel) or the normalized infection efficiency (right panel) of cells infected by the GFP-expressing KJ26 strain as measured by flow cytometry. Shown are means and SD for triplicate cultures of each clone. (E and F) Flow cytometry analysis of primary neurons transduced with the empty pTM942 vector (mCherry alone) or with the *Apol9b*-expressing vector and infected for 24 h with KJ26. Representative FACS data (E) and histograms showing means and SD of overall infection efficiencies in neurons from a typical triplicate-infection experiment (F). (G and H) Infectious virus production ($TCID_{50}$) (G) and replication of TMEV (RT-qPCR) (H) in mock-transduced neurons and in neurons transduced with the empty lentiviral vector or with the lentiviral vector expressing *ApoL9b* at different times after infection with virus KJ26.

Lentiviral vectors coexpressing an shRNA targeting the 3′ UTR of *Apol9b* and mCherry (pMK75) or expressing mCherry alone (pMK84) were used to transduce L929 cells. One week after transduction, cells were mock treated or treated for 24 h with 0.5 or 1 U/ml of IFN-β and then infected for 10 h with 1 PFU per cell of KJ26. Cells were analyzed by flow cytometry to test whether viral replication (GFP fluorescence) was increased in transduced cells (mCherry fluorescence). As shown in Fig. 8, knocking down

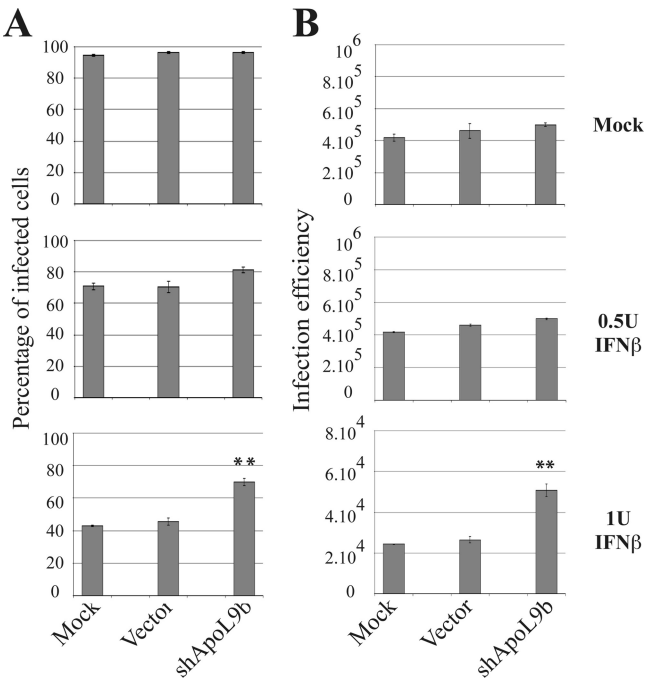

FIG 8 *Apol9b* contribution to antiviral activity in IFN-treated cells. Histograms show the percentage of infected cells (A) and normalized infection efficiency (B), as determined by FACS, in L929 cells that were mock transduced or transduced with the empty pMK84 vector or with the same vector expressing the shRNA targeting *Apol9b*. Cells were treated with low doses of IFN-β (mock, 0.5, or 1 unit/ml) 24 h prior to infection with KJ7.

Apol9b in cells that were not treated with IFN had little impact on viral replication, as expected from the fact that *Apol9b* is hardly expressed in these conditions. In cells treated with 0.5 or 1 U/ml of IFN-β, knocking down ApoL9 expression significantly increased infection efficiency.

DISCUSSION

Our data show that primary mouse neurons treated with type-I IFN acquire a surprisingly weak resistance to infection by neurotropic viruses such as Theiler's murine encephalomyelitis virus (TMEV) or vesicular stomatitis virus (VSV). Two factors likely account for the weak resistance of neurons: the heterogeneity of their responsiveness to IFN and the altered profile of ISG induction in these cells.

Our data show that basal ISG expression in untreated primary neurons is about 10-fold lower than in fibroblasts. This observation is in agreement with the reported lower ISG expression observed in the CNS than in other tissues of mice (36). Since some ISG, such as STAT1, are critical to mediate the IFN response, it is tempting to speculate that a proportion of neurons do not express enough STAT1 prior to IFN treatment to reach the threshold of responsiveness. A similar observation was recently made with rat hippocampal neurons, which turned out to be even less responsive than mouse neurons (10).

On the other hand, responsiveness of neurons to IFN may be influenced by their maturity. Neuron maturation was reported to affect their susceptibility to infection with Semliki forest virus (37). *In vivo*, maturation of the CNS also affected ISG expression after Sindbis virus infection (38). In our experiments, DIV12 neurons did not appear to be better protected by IFN treatment than DIV6 neurons. However, we cannot exclude that part of the neurons in the culture kept an immature phenotype and were therefore more susceptible to viral infection. Yet primary neurons are the first example of IFN-treated cells that keep such a high susceptibility to viral infection.

Interestingly, following IFN treatment and subsequent TMEV infection, neurons that responded to IFN by expressing Mx1 were hardly more protected than Mx1-negative cells. We hypothesized that the high susceptibility of IFN-treated neurons to TMEV infection could stem from an altered ISG response in these cells. Our transcriptomic analysis identified 15 genes that were upregulated in fibroblasts by IFN treatment but that were much less expressed in neurons. Among them, *Lgals3bp* was already documented for its antiviral activity. Expression of this gene was reported to decrease replication of yellow fever virus (YFV), Chikungunia virus (CHIKV), and West Nile virus (WNV) in STAT1-KO fibroblasts but to increase human immunodeficiency virus (HIV) infection in T cells (39). The antiviral activity of other ISG, such as *Lgals9*, *Ifi35*, *Dhx58*, and *Sp100*, was also reported (39–41). Our screen failed to detect a significant antiviral effect of these genes on TMEV infection. This might be the consequence of the target specificity of these ISG. We cannot exclude, however, that a weak effect of these genes on TMEV replication went undetected in our screening procedure. *Dhx58*, which encodes Lgp2, had no direct antiviral activity in our assay. However, Lgp2 has been shown to regulate MAVS-dependent IFN expression after viral infection (41). This gene is thus an important regulator of ISG expression and its absence in neurons could contribute to the high susceptibility of these cells to viral infection. Other ISG that are weakly expressed in neurons were previously described for their cytostatic activity (*Slfn2*) (42) or for their role in sensing cytoplasmic DNA (*Ifi200* family members) (43).

Apol9b showed a strong antiviral activity against TMEV infection in L929 fibroblasts and a modest but significant activity when expressed in primary neurons. Interestingly, knocking down *Apol9b* expression significantly increased TMEV replication in L929 cells treated with low doses of IFN-β, suggesting that the contribution of *Apol9b* to resistance against TMEV is not negligible.

The ApoL family is highly conserved across species (44). So far, only human ApoL1 and ApoL6 have been characterized. ApoL1 is a secreted protein protective against trypanosomiasis (45). Other members of the ApoL family are predicted to lack a signal peptide, and it is unclear whether they are secreted. Human ApoL6 was reported to promote apoptosis and to inhibit autophagy (46, 47), both of which might affect viral replication. In a broad ISG screen for antiviral activity, Schoggins et al. (39) observed an antiviral activity for several members of the human ApoL family. ApoL1, -L2, -L3, and -L6 restricted hepatitis C virus (HCV) infection in human Huh-7 cells. ApoL1, -L2, and -L6 restricted Venezuelan equine encephalitis virus (VEEV) infection in human *STAT1*$^{-/-}$ fibroblasts. ApoL1 also restricted WNV infection in *STAT1*$^{-/-}$ fibroblasts but increased YFV infection in these cells and HIV infection in T cells. Taken together, these data indicate that human ApoL family members are widely implicated in the defense against various viruses. However, the mode of action of these apolipoproteins is largely unknown.

In conclusion, our data show that primary mouse neurons respond in a heterogeneous manner to IFN. Moreover, some ISG

that are strongly upregulated in fibroblasts are little or not expressed in neurons. Among these genes, *Apol9b* is a novel antiviral ISG that may contribute to the surprising susceptibility of IFN-treated neurons to viral infection.

ACKNOWLEDGMENTS

We thank Martin Schwemmle and Peter Stäheli for critical readings of the manuscript. We are grateful to Stéphane Messe and Muriel Minet for expert technical assistance. We are indebted to Martine Soudant and Uwe Maskos (Unité Récepteurs et Cognition, Institut Pasteur, Paris), who introduced us to the primary neuron culture technique and to Nicolas Dauguet (Ludwig Institute for Cancer Research, Brussels) for his kind and professional help in flow cytometry.

M.K., S.P. and A.D.C. were recipients of fellowships from the FRIA. M.K. was further supported by a fellowship from the Faculty of Medicine (University of Louvain). This work was supported by the DIANE convention of the Belgian Walloon Region, by ARC (Communauté Française de Belgique), and by FRSM (Fonds National de la Recherche Médicale convention 3.4576.08 and Crédit aux Chercheurs).

REFERENCES

1. **Griffin DE, Metcalf T.** 2011. Clearance of virus infection from the CNS. Curr. Opin. Virol. **1:**216–221. http://dx.doi.org/10.1016/j.coviro.2011.05.021.
2. **Paul S, Ricour C, Sommereyns C, Sorgeloos F, Michiels T.** 2007. Type I interferon response in the central nervous system. Biochimie **89:**770–778. http://dx.doi.org/10.1016/j.biochi.2007.02.009.
3. **Sorgeloos F, Kreit M, Hermant P, Lardinois C, Michiels T.** 2013. Antiviral type I and type III interferon responses in the central nervous system. Viruses **5:**834–857. http://dx.doi.org/10.3390/v5030834.
4. **Casrouge A, Zhang SY, Eidenschenk C, Jouanguy E, Puel A, Yang K, Alcais A, Picard C, Mahfoufi N, Nicolas N, Lorenzo L, Plancoulaine S, Senechal B, Geissmann F, Tabeta K, Hoebe K, Du X, Miller RL, Heron B, Mignot C, de Villemeur TB, Lebon P, Dulac O, Rozenberg F, Beutler B, Tardieu M, Abel L, Casanova JL.** 2006. Herpes simplex virus encephalitis in human UNC-93B deficiency. Science **314:**308–312. http://dx.doi.org/10.1126/science.1128346.
5. **Sancho-Shimizu V, Perez de Diego R, Jouanguy E, Zhang SY, Casanova JL.** 2011. Inborn errors of anti-viral interferon immunity in humans. Curr. Opin. Virol. **1:**487–496. http://dx.doi.org/10.1016/j.coviro.2011.10.016.
6. **Daffis S, Samuel MA, Suthar MS, Gale M, Jr, Diamond MS.** 2008. Toll-like receptor 3 has a protective role against West Nile virus infection. J. Virol. **82:**10349–10358. http://dx.doi.org/10.1128/JVI.00935-08.
7. **Delhaye S, Paul S, Blakqori G, Minet M, Weber F, Staeheli P, Michiels T.** 2006. Neurons produce type I interferon during viral encephalitis. Proc. Natl. Acad. Sci. U. S. A. **103:**7835–7840. http://dx.doi.org/10.1073/pnas.0602460103.
8. **Préhaud C, Megret F, Lafage M, Lafon M.** 2005. Virus infection switches TLR-3-positive human neurons to become strong producers of beta interferon. J. Virol. **79:**12893–12904. http://dx.doi.org/10.1128/JVI.79.20.12893-12904.2005.
9. **Wang J, Campbell IL.** 2005. Innate STAT1-dependent genomic response of neurons to the antiviral cytokine alpha interferon. J. Virol. **79:**8295–8302. http://dx.doi.org/10.1128/JVI.79.13.8295-8302.2005.
10. **Samuel MA, Whitby K, Keller BC, Marri A, Barchet W, Williams BR, Silverman RH, Gale M, Jr, Diamond MS.** 2006. PKR and RNase L contribute to protection against lethal West Nile Virus infection by controlling early viral spread in the periphery and replication in neurons. J. Virol. **80:**7009–7019. http://dx.doi.org/10.1128/JVI.00489-06.
11. **Kallfass C, Ackerman A, Lienenklaus S, Weiss S, Heimrich B, Staeheli P.** 2012. Visualizing production of beta interferon by astrocytes and microglia in brain of la crosse virus-infected mice. J. Virol. **86:**11223–11230. http://dx.doi.org/10.1128/JVI.01093-12.
12. **Lin CC, Wu YJ, Heimrich B, Schwemmle M.** 2013. Absence of a robust innate immune response in rat neurons facilitates persistent infection of Borna disease virus in neuronal tissue. Cell. Mol. Life Sci. **70:**4399–4410. http://dx.doi.org/10.1007/s00018-013-1402-5.
13. **Staeheli P, Sentandreu M, Pagenstecher A, Hausmann J.** 2001. Alpha/beta interferon promotes transcription and inhibits replication of Borna disease virus in persistently infected cells. J. Virol. **75:**8216–8223. http://dx.doi.org/10.1128/JVI.75.17.8216-8223.2001.
14. **Cho H, Proll SC, Szretter KJ, Katze MG, Gale M, Jr, Diamond MS.** 2013. Differential innate immune response programs in neuronal subtypes determine susceptibility to infection in the brain by positive-stranded RNA viruses. Nat. Med. **19:**458–464. http://dx.doi.org/10.1038/nm.3108.
15. **Horisberger MA, Staeheli P, Haller O.** 1983. Interferon induces a unique protein in mouse cells bearing a gene for resistance to influenza virus. Proc. Natl. Acad. Sci. U. S. A. **80:**1910–1914. http://dx.doi.org/10.1073/pnas.80.7.1910.
16. **Johnson L, Mercer K, Greenbaum D, Bronson RT, Crowley D, Tuveson DA, Jacks T.** 2001. Somatic activation of the K-ras oncogene causes early onset lung cancer in mice. Nature **410:**1111–1116. http://dx.doi.org/10.1038/35074129.
17. **Wislez M, Spencer ML, Izzo JG, Juroske DM, Balhara K, Cody DD, Price RE, Hittelman WN, Wistuba II, Kurie JM.** 2005. Inhibition of mammalian target of rapamycin reverses alveolar epithelial neoplasia induced by oncogenic K-ras. Cancer Res. **65:**3226–3235. http://dx.doi.org/10.1158/0008-5472.CAN-04-4420.
18. **DuBridge RB, Tang P, Hsia HC, Leong PM, Miller JH, Calos MP.** 1987. Analysis of mutation in human cells by using an Epstein-Barr virus shuttle system. Mol. Cell. Biol. **7:**379–387.
19. **Banker GA, Cowan WM.** 1977. Rat hippocampal neurons in dispersed cell culture. Brain Res. **126:**397–425. http://dx.doi.org/10.1016/0006-8993(77)90594-7.
20. **Fath T, Ke YD, Gunning P, Gotz J, Ittner LM.** 2009. Primary support cultures of hippocampal and substantia nigra neurons. Nat. Protoc. **4:**78–85. http://dx.doi.org/10.1038/nprot.2008.199.
21. **Hermant P, Francius C, Clotman F, Michiels T.** 2013. IFN-ε is constitutively expressed by cells of the reproductive tract and is inefficiently secreted by fibroblasts and cell lines. PLoS One **8:**e71320. http://dx.doi.org/10.1371/journal.pone.0071320.
22. **van Pesch V, Lanaya H, Renauld JC, Michiels T.** 2004. Characterization of the murine alpha interferon gene family. J. Virol. **78:**8219–8228. http://dx.doi.org/10.1128/JVI.78.15.8219-8228.2004.
23. **van Pesch V, Michiels T.** 2003. Characterization of interferon-alpha 13, a novel constitutive murine interferon-alpha subtype. J. Biol. Chem. **278:**46321–46328. http://dx.doi.org/10.1074/jbc.M302554200.
24. **Daniels JB, Pappenheimer AM, Richardson S.** 1952. Observations on encephalomyelitis of mice (DA strain). J. Exp. Med. **96:**517–530. http://dx.doi.org/10.1084/jem.96.6.517.
25. **Theiler M, Gard S.** 1940. Encephalomyelitis of mice. I. Characteristics and pathogenesis of the virus. J. Exp. Med. **72:**49–67.
26. **Michiels T, Dejong V, Rodrigus R, Shaw-Jackson C.** 1997. Protein 2A is not required for Theiler's virus replication. J. Virol. **71:**9549–9556.
27. **Tangy F, McAllister A, Brahic M.** 1989. Molecular cloning of the complete genome of strain GDVII of Theiler's virus and production of infectious transcripts. J. Virol. **63:**1101–1106.
28. **van Pesch V, van Eyll O, Michiels T.** 2001. The leader protein of Theiler's virus inhibits immediate-early alpha/beta interferon production. J. Virol. **75:**7811–7817. http://dx.doi.org/10.1128/JVI.75.17.7811-7817.2001.
29. **Jnaoui K, Michiels T.** 1998. Adaptation of Theiler's virus to L929 cells: mutations in the putative receptor binding site on the capsid map to neutralization sites and modulate viral persistence. Virology **244:**397–404. http://dx.doi.org/10.1006/viro.1998.9134.
30. **Follenzi A, Ailles LE, Bakovic S, Geuna M, Naldini L.** 2000. Gene transfer by lentiviral vectors is limited by nuclear translocation and rescued by HIV-1 pol sequences. Nat. Genet. **25:**217–222. http://dx.doi.org/10.1038/76095.
31. **Shaw-Jackson C, Michiels T.** 1999. Absence of internal ribosome entry site-mediated tissue specificity in the translation of a bicistronic transgene. J. Virol. **73:**2729–2738.
32. **Moffat J, Grueneberg DA, Yang X, Kim SY, Kloepfer AM, Hinkle G, Piqani B, Eisenhaure TM, Luo B, Grenier JK, Carpenter AE, Foo SY, Stewart SA, Stockwell BR, Hacohen N, Hahn WC, Lander ES, Sabatini DM, Root DE.** 2006. A lentiviral RNAi library for human and mouse genes applied to an arrayed viral high-content screen. Cell **124:**1283–1298. http://dx.doi.org/10.1016/j.cell.2006.01.040.
33. **Paul S, Michiels T.** 2006. Cardiovirus leader proteins are functionally interchangeable and have evolved to adapt to virus replication fitness. J. Gen. Virol. **87:**1237–1246. http://dx.doi.org/10.1099/vir.0.81642-0.
34. **Meier E, Fah J, Grob MS, End R, Staeheli P, Haller O.** 1988. A family of

interferon-induced Mx-related mRNAs encodes cytoplasmic and nuclear proteins in rat cells. J. Virol. **62:**2386–2393.
35. **Burdeinick-Kerr R, Griffin DE.** 2005. Gamma interferon-dependent, non-cytolytic clearance of Sindbis virus infection from neurons in vitro. J. Virol. **79:**5374–5385. http://dx.doi.org/10.1128/JVI.79.9.5374-5385.2005.
36. **Ida-Hosonuma M, Iwasaki T, Yoshikawa T, Nagata N, Sato Y, Sata T, Yoneyama M, Fujita T, Taya C, Yonekawa H, Koike S.** 2005. The alpha/beta interferon response controls tissue tropism and pathogenicity of poliovirus. J. Virol. **79:**4460–4469. http://dx.doi.org/10.1128/JVI.79.7.4460-4469.2005.
37. **Oliver KR, Scallan MF, Dyson H, Fazakerley JK.** 1997. Susceptibility to a neurotropic virus and its changing distribution in the developing brain is a function of CNS maturity. J. Neurovirol. **3:**38–48. http://dx.doi.org/10.3109/13550289709015791.
38. **Labrada L, Liang XH, Zheng W, Johnston C, Levine B.** 2002. Age-dependent resistance to lethal alphavirus encephalitis in mice: analysis of gene expression in the central nervous system and identification of a novel interferon-inducible protective gene, mouse ISG12. J. Virol. **76:**11688–11703. http://dx.doi.org/10.1128/JVI.76.22.11688-11703.2002.
39. **Schoggins JW, Wilson SJ, Panis M, Murphy MY, Jones CT, Bieniasz P, Rice CM.** 2011. A diverse range of gene products are effectors of the type I interferon antiviral response. Nature **472:**481–485. http://dx.doi.org/10.1038/nature09907.
40. **Adler M, Tavalai N, Muller R, Stamminger T.** 2011. Human cytomegalovirus immediate-early gene expression is restricted by the nuclear domain 10 component Sp100. J. Gen. Virol. **92:**1532–1538. http://dx.doi.org/10.1099/vir.0.030981-0.
41. **Satoh T, Kato H, Kumagai Y, Yoneyama M, Sato S, Matsushita K, Tsujimura T, Fujita T, Akira S, Takeuchi O.** 2010. LGP2 is a positive regulator of RIG-I- and MDA5-mediated antiviral responses. Proc. Natl. Acad. Sci. U. S. A. **107:**1512–1517. http://dx.doi.org/10.1073/pnas.0912986107.
42. **Katsoulidis E, Carayol N, Woodard J, Konieczna I, Majchrzak-Kita B, Jordan A, Sassano A, Eklund EA, Fish EN, Platanias LC.** 2009. Role of Schlafen 2 (SLFN2) in the generation of interferon alpha-induced growth inhibitory responses. J. Biol. Chem. **284:**25051–25064. http://dx.doi.org/10.1074/jbc.M109.030445.
43. **Choubey D, Duan X, Dickerson E, Ponomareva L, Panchanathan R, Shen H, Srivastava R.** 2010. Interferon-inducible p200-family proteins as novel sensors of cytoplasmic DNA: role in inflammation and autoimmunity. J. Interferon Cytokine Res. **30:**371–380. http://dx.doi.org/10.1089/jir.2009.0096.
44. **Smith EE, Malik HS.** 2009. The apolipoprotein L family of programmed cell death and immunity genes rapidly evolved in primates at discrete sites of host-pathogen interactions. Genome Res. **19:**850–858. http://dx.doi.org/10.1101/gr.085647.108.
45. **Vanhollebeke B, Nielsen MJ, Watanabe Y, Truc P, Vanhamme L, Nakajima K, Moestrup SK, Pays E.** 2007. Distinct roles of haptoglobin-related protein and apolipoprotein L-I in trypanolysis by human serum. Proc. Natl. Acad. Sci. U. S. A. **104:**4118–4123. http://dx.doi.org/10.1073/pnas.0609902104.
46. **Liu Z, Lu H, Jiang Z, Pastuszyn A, Hu CA.** 2005. Apolipoprotein l6, a novel proapoptotic Bcl-2 homology 3-only protein, induces mitochondria-mediated apoptosis in cancer cells. Mol. Cancer Res. **3:**21–31.
47. **Zhaorigetu S, Yang Z, Toma I, McCaffrey TA, Hu CA.** 2011. Apolipoprotein L6, induced in atherosclerotic lesions, promotes apoptosis and blocks Beclin 1-dependent autophagy in atherosclerotic cells. J. Biol. Chem. **286:**27389–27398. http://dx.doi.org/10.1074/jbc.M110.210245.